Available online at www.sciencedirect.com
SCIENCE DIRECT®
Bioorganic & Medicinal Chemistry 13 (2005) 2799–2808
Bioorganic & Medicinal Chemistry

Design, synthesis, and biological evaluation of folic acid targeted tetraphenylporphyrin as novel photosensitizers for selective photodynamic therapy

Raphaël Schneider,[a,*] Frédéric Schmitt,[a] Céline Frochot,[b] Yves Fort,[a] Natacha Lourette,[d] François Guillemin,[c] Jean-François Müller[d] and Muriel Barberi-Heyob[c,*]

[a]*Synthèse Organométallique et Réactivité, UMR 7565 CNRS-UHP, Faculté des Sciences, BP 239, 54506 Vandœuvre les Nancy, France*
[b]*DCPR, UMR 7630 CNRS-INPL, Groupe ENSIC, 1 Rue Grandville, 54000 Nancy, France*
[c]*Centre Alexis Vautrin-CRAN, UMR 7039 CNRS-INPL-UHP, 54511 Vandœuvre les Nancy, France*
[d]*Laboratoire de Spectrométrie de Masse et de Chimie Laser, Université de Metz 1, France*

Received 19 October 2004; revised 4 February 2005; accepted 15 February 2005

Abstract—Photodynamic therapy (PDT) is a cancer treatment involving systemic administration of a tumor-localizing photosensitizer; this, when activated by the appropriate light wavelength, interacts with molecular oxygen to form a toxic, short-lived species known as singlet oxygen, which is thought to mediate cellular death. Targeted PDT offers the opportunity of enhancing photodynamic efficiency by directly targeting diseased cells and tissues.

Two new conjugates of three components, folic acid/hexane-1,6-diamine/4-carboxyphenylporphyrine **1** and folic acid/2,2′-(ethylenedioxy)-bis-ethylamine/4-carboxyphenylporphyrine **2** were synthesized. The conjugates were characterized by ^{1}H NMR, MALDI, UV–visible spectroscopy, and fluorescence quantum yield. The targeted delivery of these photoactive compounds to KB nasopharyngeal cell line, which is one of the numerous tumor cell types that overexpress folate receptors was studied. It was found that after 24 h incubation, conjugates **1** and **2** cellular uptake was on average 7-fold higher than tetraphenylporphyrin (TPP) used as reference and that **1** and **2** cellular uptake kinetics increased steadily over the 24 h period, suggesting an active transport via receptor-mediated endocytosis. In corresponding results, conjugates **1** and **2** accumulation displayed a reduction of 70% in the presence of a competitive concentration of folic acid. Survival measurements demonstrated that KB cells were significantly more sensitive to conjugated porphyrins-mediated PDT. Under the same experimental conditions and the same photosensitizer concentration, TPP displayed no photocytotoxicity while conjugates **1** and **2** showed photodynamic activity with light dose values yielding 50% growth inhibition of 22.6 and 6.7 J/cm^2, respectively.
© 2005 Elsevier Ltd. All rights reserved.

1. Introduction

During the past two decades, there has been a great interest in research on photosensitizers as a tool for photodynamic therapy (PDT).[1] Activation of a photosensitizer by light at specific wavelengths leads to the production of singlet oxygen and radical species, resulting in direct tumor cell killing, immune inflammatory responses, and damage to the microvasculature of the tumor.[2] Most photosensitizers tested accumulate with some selectivity in tumors, but they also concentrate in normal tissues, including the skin.[3] Targeted delivery of the photosensitizer could solve these problems through an enhanced photocytotoxicity as a result of higher and more selective accumulation in the tumor cells. Targeting implies conjugation of the photoactive

Abbreviations: BSA, bovine serum albumin; Boc, *tert*-butoxycarbonyl; DCC, dicyclohexylcarbodiimide; DMF, dimethyl formamide; DMSO, dimethyl sulfoxide; FA, folic acid; GPI, glycosylphosphatidylinositol; MTT, 3-(4,5-dimethylthiazol-2-yl)-2,5-diphenyltetrazolium bromide; NHS, *N*-hydroxysuccinimide; NMR, nuclear magnetic resonance spectroscopy; PBS, phosphate buffered saline; PDT, photodynamic therapy; PEG, poly(ethylene glycol); Por-COOH, 4-carboxy- phenylporphyrin; RP-HPLC, reversed phase high performance liquid chromatography; TFA, trifluoroacetic acid; THF, tetrahydrofuran; UV, ultraviolet.

Keywords: Photodynamic therapy; Tetraphenylporphyrin; Folic acid; Photophysical properties.

* Corresponding authors. Tel.: +33 03 8359 8306; fax: +33 03 8344 7635; e-mail: m.barberi@nancy.fnclcc.fr

0968-0896/$ - see front matter © 2005 Elsevier Ltd. All rights reserved.
doi:10.1016/j.bmc.2005.02.025

compound to a tumor-seeking molecule, either directly or by the use of a carrier. Several photosensitizers have already been conjugated with antibodies directed against tumor-associated antigens. Ligands such as low-density lipoprotein, insulin, steroids, transferrin, and epidermal growth factor have all been described for ligand-based targeting of photosensitizers to cells overexpressing the receptors of these ligands.[4] In fact, alterations in receptor expression, increased levels of specific cell surface membrane lipids and proteins as well as changes in the cellular microenvironment, all occur in diseased cells. Among the different strategies via receptor-mediated delivery systems, the receptor for folic acid also constitutes a useful target for tumor-specific drug delivery because: (1) it is upregulated in many human cancers, including malignancies of the ovary, brain, kidney, breast, myeloid cells, and lung; (2) access to the folate receptor in those normal tissues that express it can be severely limited due to its location on the apical membrane of polarized epithelia; (3) folate receptor density increases as the stage/grade of the cancer worsens; and (4) the high affinity of the folate for its cell surface receptor (K_d about 10^{-10}) appears attractive.[5] Conjugation of folic acid to macromolecules has been shown to enhance their delivery to folate receptor-expressing cancer cells in vitro in almost all situations tested.[5]

Although the precise mechanism of folate receptor transport of folic acid into cells remains unresolved, it is clear that folate conjugates are taken up nondestructively by mammalian cells via receptor-mediated endocytosis.[6,7] Physiologic folates move across the plasma membrane into the cytoplasm by a specialized endocytosis mediated pathway.[8] After binding to folate receptor on the cancer cell surface, folate conjugates, regardless of size, are seen to internalize and traffic to intracellular compartments called endosomes.[7] The present study reports for the first time the conjugation between tetraphenylporphyrin (TPP) and folic acid. Porphyrins are first-generation photosensitizers that can be easily modified through a carboxyl group, which makes the compound suitable for conjugation as we recently described.[9] In this paper, we describe first the synthesis of 4-carboxyphenylporphyrin (Por-COOH)-folic acid (FA) conjugates **1** and **2** in which FA and the Por-COOH are, respectively, linked together by the end groups of 1,6-diaminohexane or 2,2′-(ethylenedioxy)-bis-(ethylamine). The photodynamic activity of conjugates **1** and **2** toward KB cells stably overexpressing the folate receptor[10] (279×10^3 folate receptors/cell) has also been evaluated.

2. Results

2.1. Chemistry

The synthesis of novel conjugates **1** and **2** is shown in Schemes 1 and 2.

We chose to attach the folate and the porphyrin to the distal ends of two linkers in order to increase the range of accessible receptor sites. A first synthetic strategy has been investigated using hexane-1,6-diamine (Scheme 1).

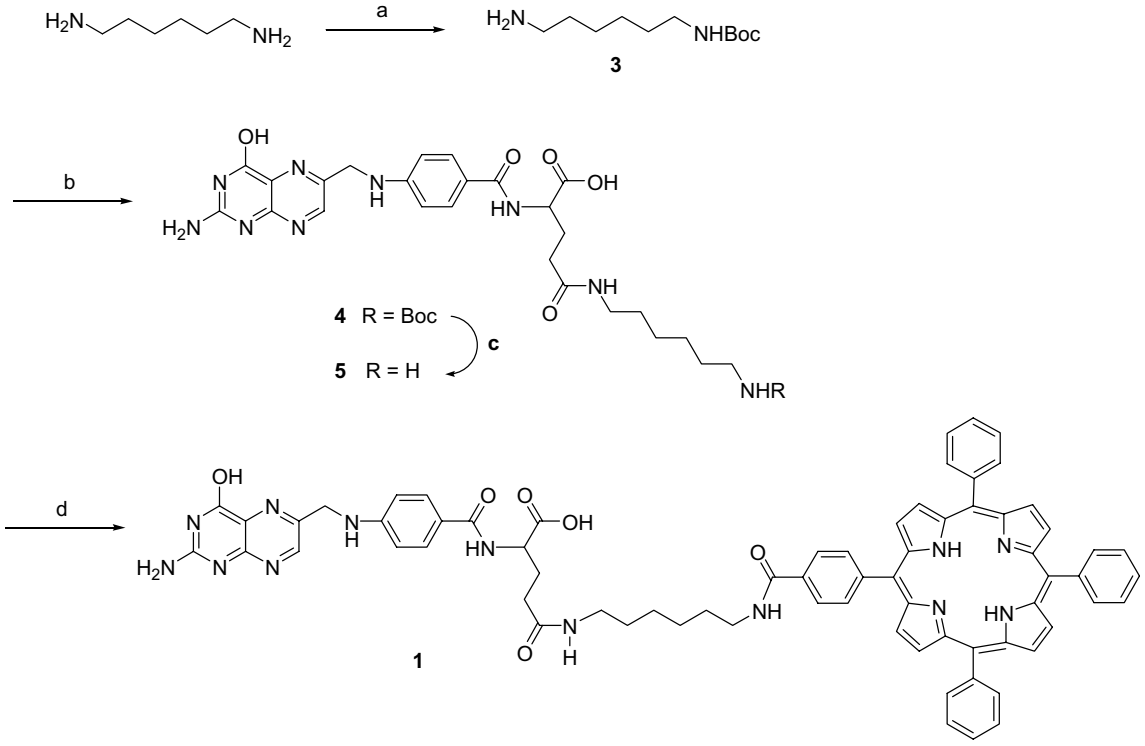

Scheme 1. Reagents and conditions: (a) Boc_2O, $CHCl_3$, 0 °C; (b) folic acid, DCC, pyridine, DMSO; (c) CF_3CO_2H, 25 °C; (d) *N*-hydroxysuccimide activated carboxyporphyrin **6**, pyridine, DMSO.

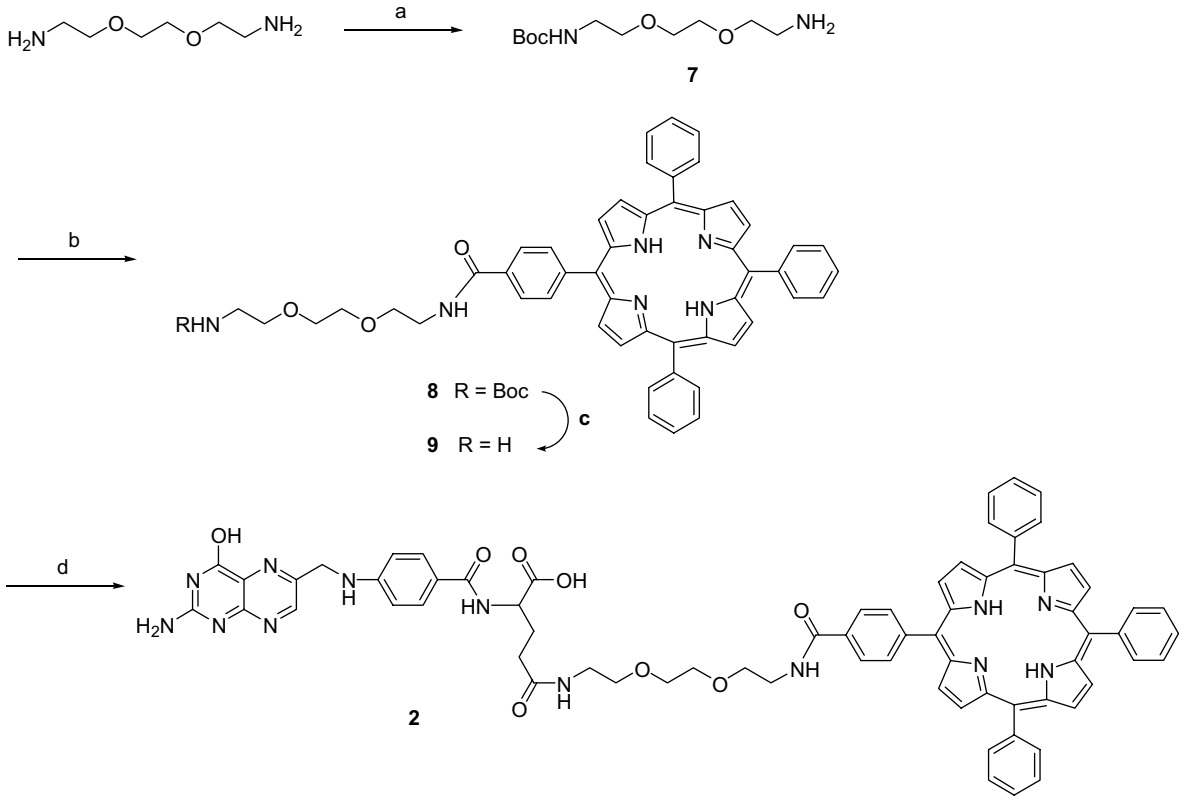

Scheme 2. Reagents and conditions: (a) Boc_2O, $CHCl_3$, 0 °C; (b) *N*-hydroxysuccinimide activated carboxyporphyrin **6**, THF; (c) CF_3CO_2H, 25 °C; (d) *N*-hydroxysuccinimide activated folic acid **10**, pyridine, DMSO.

A small PEG, 2,2′-(ethylenedioxy)-bis-ethylamine, was used in the second synthesis to increase water-solubility and biocompatibility of the conjugate (Scheme 2).

Boc-monoprotected hexane-1,6-diamine **3** was prepared following the procedure described by Stahl et al.[11] Coupling of **3** with folic acid mediated by dicyclohexylcarbodiimide (DCC) in pyridine/DMSO afforded **4**. Deprotection of the Boc group using trifluoroacetic acid (TFA) gave the amine **5**, which was in turn coupled with *N*-hydroxysuccinimide activated 4-carboxyphenylporphyrin **6** in pyridine/DMSO to afford the conjugate **1**.

As shown in Scheme 2, 2,2′-(ethylenedioxy)-bis-ethylamine, a hydrophilic linker, was used as starting material for the synthesis of conjugate **2**. One amine group was first protected with a Boc group to give **7**. Subsequent coupling with *N*-hydroxysuccinimide activated 4-carboxyphenylporphyrin **6** afforded amide **8**. The Boc protective group was removed with TFA at room temperature. Amine **9** obtained was finally coupled with *N*-hydroxysuccinimide activated folic acid **10** in pyridine/DMSO to give the conjugate **2**.

Since the folic acid molecule possesses two carboxyl groups, termed α and γ, which can act as handles for covalent attachment, it was important to determine the relative amounts of each α- and γ-carboxyl-linked conjugates in compounds **1** and **2**. Indeed, it has been demonstrated that the folate linked via its γ-carbonyl group retains a strong affinity toward its receptor, whereas its α-carbonyl derivatives are not recognized as readily.[12,13] By ^{1}H NMR and RP-HPLC, we determined that ca. 85% of conjugates **1** and **2** were linked through the γ-carboxyl group. These proportions of α- and γ-products are consistent with the previously reported results obtained by Low and Zalipsky.[14,15]

Compounds **1** and **2** were isolated as purple solids and were purified by repetitive dissolution in DMSO followed by reprecipitation in CH_2Cl_2/hexane (1/3) mixtures for biological evaluation. The structures of the purified conjugates were corroborated by ^{1}H NMR and UV–visible analysis. Finally, MALDI-TOF mass spectroscopy analysis revealed the expected mass for **1** (found, *m*/*z* = 1180.47; calcd, 1180.494) (Fig. 1A) and **2** (found, *m*/*z* = 1212.49; calcd, 1212.484) (Fig. 1B).

2.2. Photophysical properties

The absorption spectra of conjugates **1** and **2** were typical of porphyrin derivatives with a Soret band about 415 nm and a high extinction coefficient for this signal (Fig. 2 and Table 1) and four Q bands (512, 545, 590 and 650 nm; Fig. 2). The presence of folic acid residue results in a low decrease of extinction coefficients. The structure of the linker influences also the absorption properties. Thus, conjugate **1** displayed a lower extinction coefficient value at 650 nm than **2** (1266 vs 2373 M^{-1} cm^{-1}, respectively, Table 1). The fluorescence quantum yields were also slightly enhanced by the presence of folic acid. It may finally be noted that conjugates **1** and **2** showed simultaneously the fluorescence emission corresponding to folic acid at 350 nm and

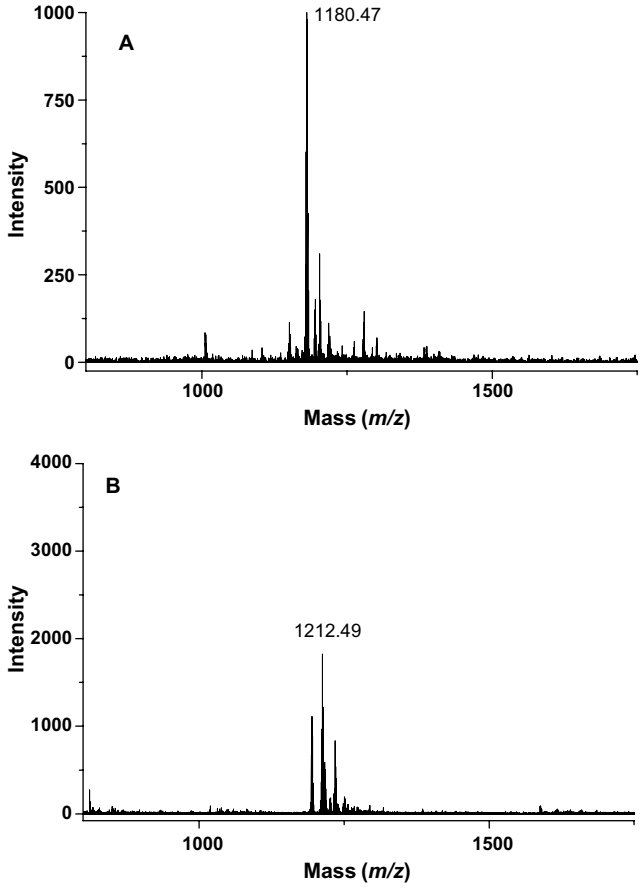

Figure 1. MALDI-TOF mass spectra of folic acid-porphyrin conjugates **1** (A), and **2** (B). The molecular ions were at 1180.47 and 1212.49, respectively.

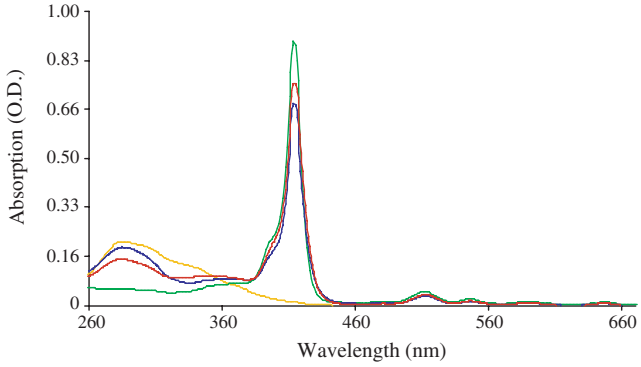

Figure 2. Absorption spectra of folic acid (—), 4-carboxyphenylporphyrin (—), conjugate **1** (—) and conjugate **2** (—) in ethanol.

Table 1. Molar extinction coefficients (ε)[a] determined at different maximum wavelengths (ε)$_\lambda$, fluorescence quantum yields (ϕ_f) of photosensitizers in ethanol

Photosensitizer	ε_{286}	ε_{414}	ε_{512}	ε_{545}	ε_{590}	ε_{650}	ϕ_f (%)
1	35,025	118,763	5823	2431	1592	1266	9.8
2	40,850	202,082	9653	4392	2868	2373	9.9

[a] Molar extinction coefficient values in M^{-1} cm^{-1}.

porphyrin typical fluorescence emission specific at 650 nm (Fig. 3).

2.3. Biological results

2.3.1. Accumulation assay. The cellular uptake of TPP, used as reference in this study, and conjugates **1** and **2** as a function of incubation time, was examined for two noncytotoxic photosensitizer concentrations (10^{-6} and 10^{-5} M, Fig. 4). The cellular accumulation of the photoactive compounds was investigated using KB cells, which overexpress folate receptors.[10] Despite a varied profile of uptake kinetics between **1** and **2** at 10^{-6} M, a statistic study using Mann–Whitney *U* test revealed that this uptake distinction was not significant (Fig. 4A). After 6 h incubation, the accumulation of folic acid-conjugated photosensitizers **1** and **2** was distinctly higher than the cellular uptake of TPP and this improvement was observed for both concentrations tested (Fig. 4A and B). The cellular uptake of conjugates **1** and **2** (10^{-5} M) after a 24 h exposure was on average about 7-fold higher than the concentration of TPP. Conjugates **1** and **2** cellular uptake increased steadily over a 24 h period, suggesting active transport via receptor-mediated endocytosis rather than nonspecific cell absorption.

2.3.2. Antiproliferative assay. MTT test was first used to evaluate the cytotoxicity of TPP, and conjugates **1** and **2** in the dark (dark cytotoxicity) for concentrations varying from 0.5 to 30.0 μM. First experiments yielding surviving cell fraction higher than 90%, demonstrated that 24 h incubation of KB cells with photoactive compounds (TPP, **1** or **2**) induced no cytotoxicity in the

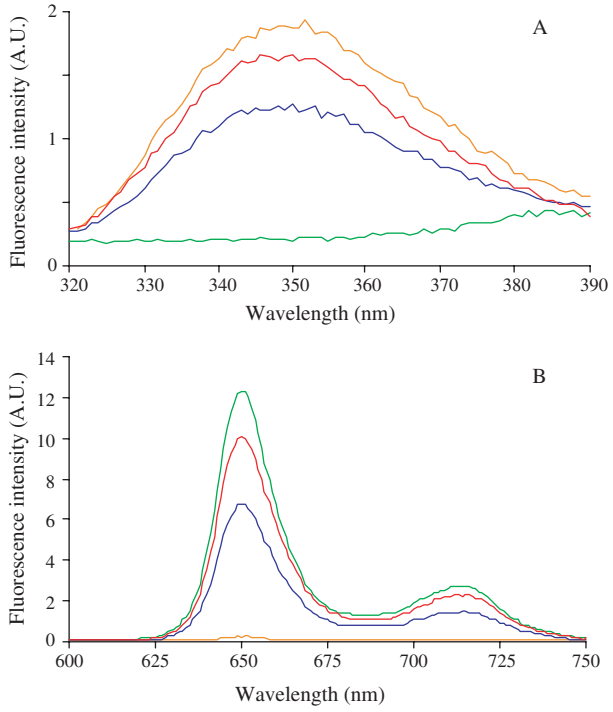

Figure 3. Fluorescence emission spectra of folic acid (—), 4-carboxyphenylporphyrin (—), conjugate **1** (—) and conjugate **2** (—) in ethanol. Excitation wavelengths were (A) 286 nm and (B) 414 nm, respectively.

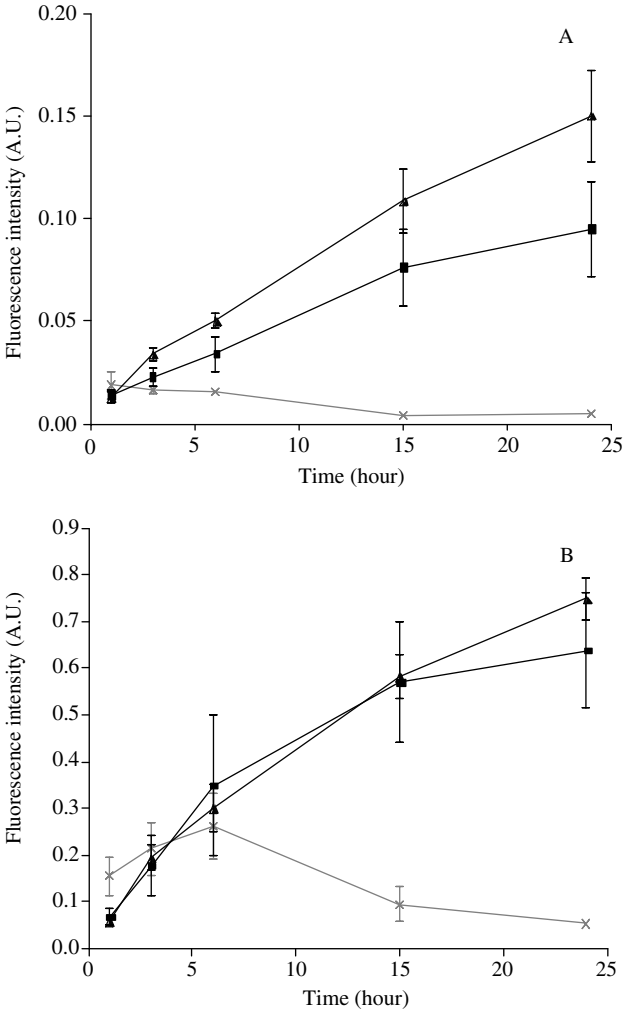

Figure 4. Uptake kinetics of TPP [gray cross] and folic acid-porphyrin conjugated **1** [square] and **2** [triangle]. KB cells were incubated with photosensitizers at (A) 10^{-6} M and (B) 10^{-5} M. Cellular fluorescence intensities were measured at 650 nm. These data represent the mean values from three independent experiments. Error bars are standard deviations.

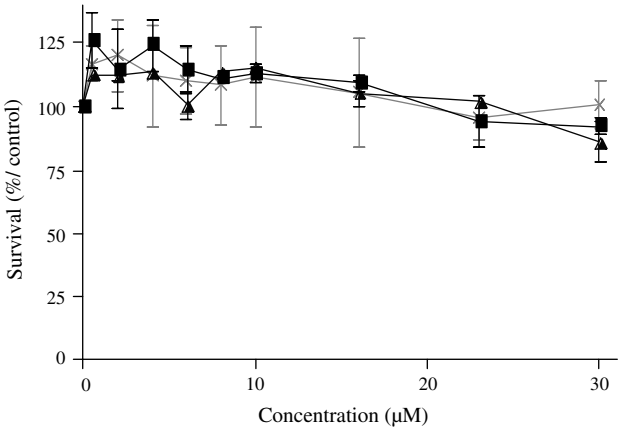

Figure 5. Concentration dependence of the cytotoxicity of TPP [gray cross], folic acid-porphyrin conjugated **1** [square] or **2** [triangle] in KB cells, as determined by an antiproliferative assay (MTT test). Data represent the mean values from three independent experiments. Error bars are standard deviations.

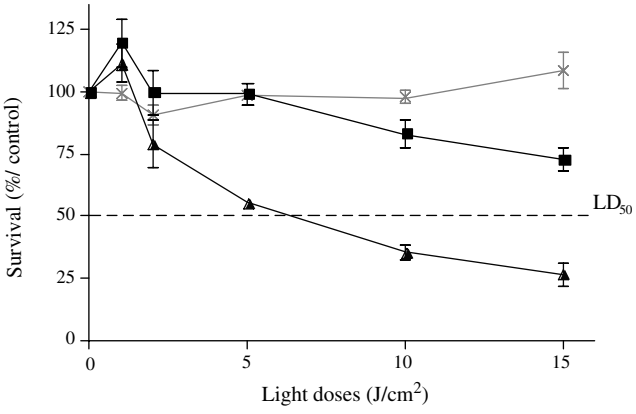

Figure 6. Measurement of photodynamic therapy sensitivity for TPP [gray cross], folic acid-porphyrin conjugated **1** [square] or **2** [triangle] in KB cells. Survival curves obtained by MTT test, were assessed for cells exposed to increasing doses of light from 1.5 to 15.0 J/cm^2 (see 'Experimental'). Cells were incubated with photosensitizers 10^{-5} M for 24 h before light treatment. Data represent the mean values from three independent experiments. Error bars are standard deviations.

absence of light exposure using MTT assay (Fig. 5). The addition of folic acid did not modify the absence of cytotoxicity measured with TPP.

2.3.3. Phototoxicity of TPP versus folic acid-conjugated photosensitizers 1 and 2. The cells were incubated with photoactive compounds and irradiated by red light as we previously described,[16] except that KB cells were exposed to the dye for 24 h at 37 °C, as the intracellular uptake kinetics demonstrated that the cellular concentrations were still improved after 24 h exposure (Fig. 4). Figure 6 shows that TPP control photosensitizer displayed no phototoxicity in our experimental conditions. On the contrary, survival measurements with MTT test demonstrated that using folic acid-conjugated **1** and **2**, the photosensitivity was improved in comparison to TPP-mediated photosensitization. Nevertheless, Figure 6 shows that only conjugate **2** exhibited a significant different photosensitivity compared to TPP. The LD_{50} values of **1** and **2** were 22.6 and 6.7 J/cm^2, respectively. Conjugate **2** was significantly more efficient (3.4-fold) compared to conjugate **1**. Despite an intracellular uptake improvement for both conjugated porphyrins, only **2**, delivered to KB cells was significantly more phototoxic than either non-conjugated porphyrin or folate-targeted porphyrin with hexane-1,6-diamine as linker.

2.3.4. Competition assays. After 24 h exposure, the accumulation of conjugates **1** and **2** was higher than the cellular uptake of non-conjugated porphyrin. Figure 7 shows that 4 mM free folic acid significantly reduced the uptake of conjugated porphyrins in KB cells ($p < 0.05$), but had no significant effect for TPP uptake. Actually, the cellular uptake of TPP was not influenced by the presence of a competitive concentration of folic acid in the incubation medium. However, despite a decrease of conjugates **1** and **2** accumulation in the presence of competing folic acid, cellular accumulation remained superior compared to TPP, leading to suggest

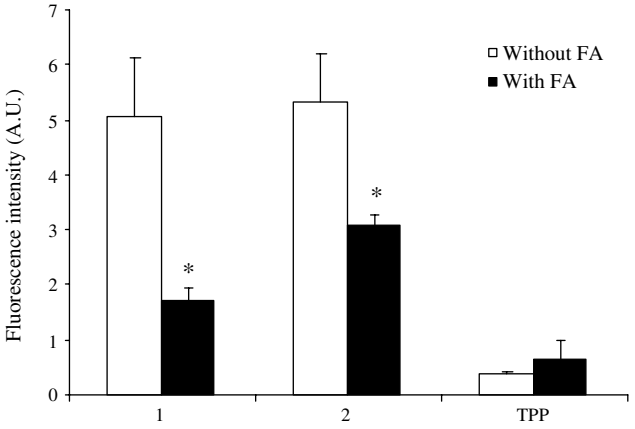

Figure 7. Intracellular concentration of the investigated compounds in KB cells in the presence or absence of folic acid. KB cells were incubated with 10^{-6} M of the photoactive compounds (**1**, **2**, or TPP) for 24 h, with or without, a competing concentration of folic acid at 4×10^{-3} M. The results are expressed as calculated intracellular concentrations (see 'Experimental'). Data represent the mean values from three independent experiments. Error bars are standard deviations. Statistically significant difference from the control without acid folic is indicated as $*p < 0.05$.

that the presence of folic acid could also increase non-specific uptake (Fig. 7).

3. Discussion

Although folic acid-mediated delivery of diverse therapeutic agents has been widely described in the literature,[6,10,14,17–21] we report herein the first conjugation between a photosensitizer and folic acid. It was anticipated that by using this strategy, a higher and selective intracellular photosensitizer concentration could be obtained, thereby enhancing the cytotoxic effect after photoactivation.

We have demonstrated that folic acid-mediated targeting of porphyrins modifies the photobiological activity of the reference molecule TPP. As seen by the extinction coefficients values (Table 1), the nature of the linker can influence photophysical properties and therefore photodynamic activity. In contrast, the affinity of folic acid for its receptor does not seem to be impaired by the nature of the linker. Thus, conjugates **1** and **2** accumulated on average about 7-fold higher than TPP after 24 h incubation using KB cells overexpressing the folate receptor (279×10^3 folate receptors/cell).[10]

Tumor cells are known to exhibit considerable variation in the number and types of receptors that they overexpress relative to healthy tissues and to other types of tumors.[22–24] The overexpression of a given receptor is often used to target photosensitizers delivery to tumor cells both in vitro and in vivo.[4] For cells such as KB cells that overexpress the folate receptor, the use of the folate-targeting ligand mediates uptake of a variety of molecules and anti-tumor agents, via the folate receptor.[25–27] The dependence of uptake on the folate receptor in KB cells was established by performing a competitive uptake assay in the presence of 4 mM free folic acid. Conjugates **1** and **2** accumulated poorly in KB cells in the presence of a competing concentration of folic acid. This amount of free folic acid is 4000-fold higher than the amount of folate introduced to the cell culture by the folic acid-conjugated porphyrins. The high concentration of free folic acid necessary to competitively inhibit folate receptor-dependent binding and uptake has been postulated to be due to the interaction between the number of folate receptors per cell, the index of cell growth, K_d value and the concentration of folate-targeting photosensitizers. It is concluded that the cellular uptake of conjugates **1** and **2** in KB nasopharyngeal carcinoma cells is folate specific and is much more potent than non-conjugated porphyrin.

The family of human folate receptors consists of three well-characterized isoforms (α, β and γ/γ′) that are identical in amino acid sequence, but distinct in their expression patterns.[28] Folate receptors α and β are both membrane-associated proteins as a consequence of their attachment to a glycosylphosphatidylinositol (GPI) membrane anchor. It is clear that folate conjugates are taken up non-destructively via receptor-mediated endocytosis. Nevertheless, there have been conflicting reports on the pathway involved in the internalization of GPI-anchored folate receptors. Early studies suggested that the folate receptor is not associated with clathrin-coated pits, but organized into submicron domains at the cell surface. These studies also suggested that the GPI anchor might be responsible for mediating receptor clustering in combination with flask-shaped membrane structures called caveolae. More recent studies seem to suggest that folate receptor is organized by its GPI anchor into receptor rich complexes in the membrane devoid of caveolae, but rich in sphingolipid and cholesterol. Regardless of the entry route, folates move across the plasma membrane via a specialized endocytosis pathway mediated by the folate receptors. As seen from the uptake kinetic profiles, cellular internalization of folic acid-conjugated TPP and reference molecule appears to involve distinct processes. Compared to conjugates **1** and **2**, the TPP uptake is a saturable process. Despite a decrease of conjugates **1** and **2** intracellular amount in the presence of a competing concentration of folic acid, the accumulation remains superior to TPP, suggesting that the presence of folic acid could also increase nonspecific uptake. These results show that passive diffusion of aggregated form could also occur for conjugates **1** and **2**. In fact, due to their chemical structure and hydrophobicity, most photosensitizers tend to aggregate in aqueous cell culture media as a result of the propensity of the hydrophobic skeleton to avoid contact with water molecules.[29] This state is one of the determining factors, which can hinder the efficacy of the drug in vivo, by decreasing its bioavailability and limiting its capacity to absorb light.[30]

For the same irradiation dose, TPP displayed no photocytotoxicity. On the contrary, use of conjugates **1** and **2** markedly increased the photodynamic effect. For a light dose of 15 J/cm^2, photodynamic activity of **1** and **2** leads to a survival fraction of about 70% and 30%,

respectively. Despite an improvement of both conjugated photosensitizers' cellular accumulation, survival measurements demonstrated that conjugate **2** was 3.4-fold more efficient than **1**. This weak **1** photocytotoxicity can be explained by the difference of light absorption at 650 nm between **1** and **2** (extinction coefficient values of 1266 vs 2373 M^{-1} cm^{-1}, respectively).

In relation to their fluorescence quantum yields, **1** and **2** could also be suggested for photomedical approaches in diagnosis. In fact, it has been known for some time that porphyrins and related compounds have the ability to accumulate in tumor tissues, and to persist there for long periods of time. Thus, conjugated porphyrin-based photosensitizers can also be proposed in the detection of cancer. Detection of autofluorescence and photosensitizer-mediated fluorescence is a promising approach to diagnose gynecologic malignancies and premalignant lesions.[31] Therefore, our new folic acid-mediated targeting promise a selective tumor-targeting and consequently, a selective diagnosis or treatment of malignant disease.

4. Conclusions

In this study, we report the first synthesis of folate-targeted porphyrins. Folic acid and 4-carboxyphenylporphyrin were conjugated using hexane-1,6-diamine or 2,2′-(ethylenedioxy)-bis-ethylamine as linkers, to produce conjugates **1** and **2**, possessing interesting fluorescence quantum yields. We have demonstrated that selective recognition of the conjugates by the folate receptors is maintained by the linking of folate to the porphyrin. By combining the tumoral-targeting ability of folic acid with the unique photophysical properties of porphyrins, we have succeeded in the design of new and highly efficient systems for photodynamic therapy. Future investigations will focus on the synthesis and the study of properties of new folate-targeted photosensitizers, displaying enhanced properties in the red spectrum.

5. Experimental

5.1. Synthesis

NMR spectra were recorded on a Brucker AM 400 spectrometer operating at 400.13 MHz for ^1H and 100.40 MHz for ^{13}C. ^1H NMR spectra are reported in units of δ with $CHCl_3$ resonance at 7.26 ppm used as the chemical shift resonance. ^{13}C NMR spectra are reported in units of δ relative to $CDCl_3$ at 77.00 ppm. Silica gel plates (Merck F_{254}) were used for thin layer chromatography. Chromatographic purification was performed with silica gel (200–400 mesh). IR spectra were recorded using NaCl. THF was distilled under nitrogen from sodium benzophenone ketyl. DMSO and DMF were distilled under nitrogen from calcium hydride before use.

5,10,15-Tri(*p*-tolyl)-20-(*p*-carboxyphenyl)porphyrin (Por-COOH) was synthesized via condensation of benzaldehyde, 4-carboxybenzaldehyde and pyrrole under acid catalysis.[32] *N*-Hydroxysuccinimide activated folic acid (NHS-folate) was prepared following the method described by Lee and Low.[17]

5.1.1. 5,10,15,Tri(*p*-tolyl)-20-(*p*-carboxyphenyl)porphyrin succinidyl ester 6. In the dark under a nitrogen atmosphere, to a solution of 5,10,15-tri(*p*-tolyl)-20-(*p*-carboxyphenyl)porphyrin (50 mg, 7.6×10^{-2} mmol) in anhydrous 1,4-dioxane (2 mL) were added *N*-hydroxysuccinimide (8.7 mg, 7.6×10^{-2} mmol) and dicyclohexylcarbodiimide (DCC) (15.7 mg, 7.6×10^{-2} mmol). The mixture was stirred 4 h at room temperature. The solvent was evaporated and the raw material purified by column chromatography using acetone/CH_2Cl_2:1/9 (v/v) as the eluent. The fractions were tested by TLC, those containing only one single spot were collected and concentrated. Compound **6** was isolated as a purple solid (52 mg, 91%); ^1H NMR ($CDCl_3$): δ 8.98–8.77 (m, 8H), 8.58 (d, $J = 8.0$ Hz, 2H), 8.42 (d, $J = 8.0$ Hz, 2H), 8.28–8.23 (m, 6H), 7.86–7.75 (m, 9H), 3.02 (br s, 4H), −2.73 (s, NH, 2H).

5.1.2. Synthesis of γ-{[*tert*-butyl *N*-(6-aminohexyl)]carbamate}folic acid 4. Under a nitrogen atmosphere at room temperature, to a solution of folic acid (FA) (1.61 g, 3.66 mmol) in anhydrous DMSO (64 mL) and pyridine (32 mL) were added the *tert*-butyl *N*-(6-aminohexyl)carbamate **3** (0.879 g, 4.03 mmol) and dicyclohexylcarbodiimide (DCC) (1.88 g, 9.15 mmol) and the mixture was stirred 18 h at room temperature. The reaction mixture was filtered and the filtrate was gradually poured into a vigorously stirred solution of dry Et_2O (1 L) cooled to 0 °C. The yellow precipitate was collected by filtration, washed with Et_2O after isolation to remove trace amounts of DMSO and dried under high vacuum to yield 2.2 g (95%) of compound **4** as a yellow solid; ^1H NMR (DMSO-d_6): δ 11.49 (br s, 1H), 8.64 (s, 1H), 7.82 (br t, 1H, NH), 7.65 (d, $J = 8.8$ Hz, 2H), 6.93 (br t, 1H, NH), 6.74 (br t, 1H, NH), 6.63 (d, $J = 8.8$ Hz, 2H), 4.49 (d, $J = 5.6$ Hz, 2H), 4.36–4.23 (m, 1H), 3.01 (td, $J = 6.0$, 6.0 Hz, 2H), 2.88 (d, $J = 6.4$ Hz, 2H), 2.29–2.15 (m, 2H), 1.98–1.82 (m, 2H), 1.41–1.16 (m, 8H), 1.36 (s, 9H); ^{13}C NMR (DMSO-d_6): δ 175.42, 172.62, 170.10, 164.66, 159.62, 154.01, 152.39, 149.38, 147.25, 127.50, 126.54, 120.17, 109.61, 75.72, 51.17, 44.61, 29.25, 27.88, 27.48, 26.90, 24.46.

5.1.3. Synthesis of γ-(6-aminohexyl)folic acid 5. Compound **4** (0.498 g, 0.78 mmol) was treated with trifluoroacetic acid (TFA) (4 mL). After been stirred at ambient temperature for 2 h, TFA was evaporated under high vacuum and the residue was taken up in anhydrous DMF. Pyridine was added dropwise until complete formation of a yellow precipitate, which was collected by filtration, washed with Et_2O and dried under vacuum to yield 421 mg (100%) of compound **5**. ^1H NMR (DMSO-d_6): δ 8.65 (s, 1H), 7.96 (m, 1H, NH), 7.84 (m, 1H, NH), 7.73 (m, 2H), 7.66 (d, $J = 7.6$ Hz, 2H), 7.32 (br s, 1H), 6.64 (d, $J = 7.6$ Hz, 2H), 4.50 (s, 2H), 4.38–4.24 (m, 1H), 3.04 (br td, 2H), 2.77 (m, 2H), 2.38–1.77 (m, 4H), 1.73–1.16 (m, 8H).

5.1.4. Synthesis of [γ-(6-aminohexyl)folic acid]-4-carboxyphenylporphyrin 1. In the dark under a nitrogen atmosphere, to a solution of 7.8 mg of **5** (1.45×10^{-2} mmol) in anhydrous DMSO (0.7 mL) and pyridine (0.3 mL) were added *N*-hydroxysuccinimide activated porphyrin **6** (10.9 mg, 1.45×10^{-2} mmol). After been stirred at ambient temperature for 24 h, the mixture was gradually poured into a vigorously stirred solution of anhydrous Et_2O (20 mL) cooled to 0 °C. The dark red precipitate obtained was collected by filtration, washed with Et_2O and CH_2Cl_2 and dried under high vacuum to yield 6.5 mg (34%) of compound **1**; ^{1}H NMR (DMSO-d_6): δ 8.89–8.77 (m, 7H), 8.64 (s, 1H), 8.32–8.17 (m, 7H), 7.90–7.78 (m, 13H), 7.66 (d, J = 8.8 Hz, 2H), 6.95 (br s, 2H, NH), 6.64 (d, J = 8.8 Hz, 2H), 4.48 (d, J = 6.0 Hz, 2H), 4.93–4.75 (m, 1H), 3.04 (br td, 2H), 2.76 (d, J = 6.2 Hz, 2H), 2.08–1.60 (m, 4H), 1.56–1.18 (m, 8H), −2.96 (s, 2H, NH); UV–vis$_{(MeOH)}$: 286 nm (ε = 35,025), 414 nm (ε = 118,763), 512 nm (ε = 5823), 545 nm (ε = 2431), 590 nm (ε = 1592), 650 nm (ε = 1266).

5.1.5. *tert*-Butyl *N*-{2-[2-(2-aminoethoxy)ethoxy]ethyl}-carbamate 7. Under a nitrogen atmosphere, to a solution of 2,2′-(ethylenedioxy)-bis-(ethylamine) (14.8 g, 100 mmol) in anhydrous $CHCl_3$ (100 mL) cooled to 0 °C was added dropwise di-*tert*-butyldicarbonate (Boc_2O) (2.18 g, 10 mmol) in 50 mL $CHCl_3$. After been stirred 24 h at room temperature, the solvent is evaporated under vacuum. The thick oil obtained is taken up in CH_2Cl_2 (100 mL). The organic layer is successively washed with saturated aqueous NaCl (2 × 50 mL), water (50 mL), dried over anhydrous $MgSO_4$ and concentrated in vacuo to afford 2.20 g (89%) of crude **7**. This material was used without further purification; ^{1}H NMR ($CDCl_3$): δ 5.15 (br s, 1H, NH), 3.63–3.51 (m, 8H), 3.31 (td, J = 5.0, 5.0 Hz, 2H), 2.88 (t, J = 4.8 Hz, 2H), 1.45 (s, 9H), 1.40 (s, 2H, NH_2); ^{13}C NMR ($CDCl_3$): δ 155.42, 78.13, 72.80, 69.63, 41.08, 39.67, 27.77; IR (NaCl) (ν, cm^{-1}): 3355, 2969, 2946, 2868, 1700, 1532, 1278, 1258, 1169, 1099.

5.1.6. Synthesis of *tert*-butyl *N*-{2-[2-(2-aminoethoxy)ethoxy]ethyl carbamate}-4-carboxyphenyl porphyrin 8. In the dark under a nitrogen atmosphere, to a solution of 26.2 mg (1.06×10^{-1} mmol) of compound **7** in anhydrous THF (1 mL) was added *N*-hydroxysuccinimide activated porphyrin **6** (160 mg, 2.12×10^{-1} mmol). After been stirred at ambient temperature for 18 h, the reaction mixture was adsorbed on silica gel and concentrated in vacuo. Column chromatography using acetone/CH_2Cl_2/hexane:1/4/5 (v/v/v) as the eluant afforded 71 mg (75%) of compound **8**. ^{1}H NMR ($CDCl_3$): δ 8.81–8.67 (m, 8H), 8.22–8.02 (m, 10H), 7.72–7.53 (m,9H), 6.96 (br s, 1H, NH), 4.95 (br s, 1H, NH), 3.82–3.71 (m, 4H), 3.71–3.59 (m, 4H), 3.52 (br td, 2H), 3.27 (br td, 2H), 1.32 (s, 9H), −2,86 (s, 2H, NH).

5.1.7. Synthesis of *N*-{2-[2-(2-aminoethoxy)ethoxy]ethyl}-4-carboxyphenylporphyrin 9. In the dark under a nitrogen atmosphere, compound **8** (72.7 mg, 0.08 mmol) was treated with trifluoroacetic acid (TFA) (2 mL). After been stirred at ambient temperature for 2 h, TFA was evaporated under high vacuum. The residue was diluted in CH_2Cl_2 and anhydrous potassium carbonate was added until a color change from green to purple red. After filtration, the organic layer was concentrated to afford 60 mg (95%) of compound **9**. This material was used without further purification; ^{1}H NMR ($CDCl_3$): δ 8.78–8.64 (m, 8H), 8.18 (d, J = 7.6 Hz, 2H), 8.12–8.01 (m, 8H), 7.67–7.50 (m, 9H), 7.23 (br t, 1H, NH), 3.77–3.63 (m, 4H), 3.63–3.49 (m, 4H), 3.43 (t, J = 4.8 Hz, 2H), 2.78 (br s, 2H), 1.92 (br t, 2H), −2.87 (s, 2H, NH).

5.1.8. Synthesis of {γ-{*N*-{2-[2-(2-aminoethoxy)ethoxy]ethyl}folic acid}}-4-carboxyphenylporphyrin 2. In the dark under a nitrogen atmosphere, to a solution of *N*-hydroxysuccinimide activated folic acid **10**[17] (10.5 mg, 0.019 mmol) in anhydrous DMSO (0.7 mL) and pyridine (0.3 mL) was added compound **9** (15.3 mg, 0.019 mmol). After been stirred at ambient temperature for 24 h, the mixture was gradually poured into a vigorously stirred solution of anhydrous Et_2O (20 mL) cooled to 0 °C. The dark red precipitate obtained was collected by filtration, washed with Et_2O and CH_2Cl_2 and dried under high vacuum to yield 6.5 mg (28%) of compound **2**; ^{1}H NMR (DMSO-d_6): δ 8.90–8.75 (m, 7H), 8.65 (s, 1H), 8.36–8.12 (m, 7H), 7.88–7.75 (m, 13H), 7.65 (d, J = 8.8 Hz, 2H), 7.43 (t, J = 6.2 Hz, 1H, NH), 6.94 (br s, 2H, NH), 6.60 (d, J = 8.8 Hz, 2H), 4.49 (br s, 2H), 4.45–4.38 (m, 1H), 3.72–3.48 (m, 12H), 2.11–1.76 (m, 4H), −2.93 (s, 2H, NH); UV–vis$_{(MeOH)}$: 286 nm (ε = 40,850), 414 nm (ε = 202,082), 512 nm (ε = 9653), 545 nm (ε = 4392), 590 nm (ε = 2862), 650 nm (ε = 2373).

5.2. Mass spectrometry analysis

MALDI sample preparation: A saturated α-cyano-4-hydroxy-*trans*-cinnamic acid (CHCA) solution, in 50/50 EtOH/H_2O, 0.01% of trifluoroacetic acid (TFA), and 1 μL of sample were spotted on the stainless steel MALDI targets. The molar ratio of analyte to matrix was 1:10^4. The solvent was evaporated prior to insertion in the source. Mass spectra were acquired over the range 0–3000 Da.

5.3. Time of flight mass spectrometer (TOFMS)

Analyses were performed on a Bruker Reflex IV time-of-flight mass spectrometer (Bruker-Daltonic, Bremen Germany) equipped with the SCOUT 384 probe ion source. The system uses a pulsed nitrogen laser (337 nm, model VSL-337ND, Laser Science Inc., Boston, MA) with energy of 400 μJ/pulse. The ions were accelerated under delayed extraction conditions (200 ns) in the positive mode with an acceleration voltage of 20 kV and a reflector voltage of 23 kV. The detector signals were amplified and transferred to the XACQ program on a SUN work station (Sun Microsystems Inc. Palo Alto, CA). Spectra were processed with the XMass 5.1 program (Bruker Daltonics, Bremen, Germany). External calibration of MALDI mass spectra was carried out using sodic and potassic distribution of PEG 600.

5.4. General procedure for in vitro experiments

Cell culture conditions: Cell culture materials were purchased from Costar (Dutscher, Brumath, France), culture media and additives from Life Technologies (Gibco BRL, Cergy-Pontoise, France), except for fetal calf serum, which was obtained from Costar. All other chemicals were purchased from Sigma (Quentin Fallavier, France). KB, head and neck carcinoma cell line, was obtained from Professor A. Hanauske (Munich University, Germany) as part of the EORTC Preclinical Therapeutic Models Group exchange program.

As we previously described,[33] KB cells were grown in 75 cm^2 plastic tissue culture flasks in RPMI 1640 medium supplemented with 9% heat inactivated fetal calf serum, penicillin (100 i.u. mL^{-1}), streptomycin (100 μg mL^{-1}) in a 37 °C, 5% CO_2 atmosphere.

5.5. Photosensitizers uptake

Cells (5×10^4 cells mL^{-1}) were inoculated in 25 cm^2 plastic tissue culture flasks and incubated for 72 h for proper attachment to the substratum. The cells were then exposed to photosensitizers (**1**, **2**, or TPP at 10^{-5} or 10^{-6} M) in RPMI supplemented with 9% of bovine serum albumin (BSA) from 2 to 24 h. After incubation with the photosensitizers, the cells were washed twice in phosphate buffered saline (PBS), harvested by enzymatic disaggregation (Trypsin-EDTA). After, the cells were washed in ice-cold PBS using centrifugation (200 g) and the fluorescence emission from the drug-loaded cells was measured in 1.5 mL ethanol solution. The fluorescence intensity of each sample was normalized to cell concentration.

5.6. Fluorescence

Steady-state emission spectra in solution and drug-loaded cells were carried out using a 10 mm-pathlength quartz *and absorption measurements* cuvette in a computer-controlled Perkin–Elmer LS5OB luminescence spectrometer equipped with a xenon discharge lamp and a red-sensitive photomultiplier (Hamamatsu R928). Spectra were collected for wavelengths ranging from 600 to 750 nm (the bandpass of both excitation and emission slits were 2.5 nm, in case of drug-loaded cells 2.5 and 5.0 mm, respectively; excitation wavelength was 411 nm; photomultiplier voltage 770 V).

For all measurements, front surface accessories (Perkin–Elmer L225 9051) have been used, providing small angle (45°) front surface excitation geometry. All absorption spectra were recorded with a Perkin–Elmer Lambda Bio spectrophotometer, using a 10 mm quartz cuvette.

5.7. Cytotoxicity assays

Cell survival was measured using MTT assay. Before performing growth inhibition assays, we examined the linearity of the MTT assay with increasing number of KB cells plated between 10^3 to 5×10^6 cells mL^{-1} and found quite satisfactory results ($r > 0.995$). Briefly, cells were seeded at the initial density of 2×10^4 cells mL^{-1} in 96-well microtitration plates. Forty-eight hours after plating, cells were exposed for 24 h to photosensitizers (TPP, **1** or **2**) for concentrations varying from 0.5 to 30 μM. After 24 h incubation at 37 °C, the medium was removed, cells were washed three times with cold PBS and fresh RPMI was added. Each concentration was tested in sextuplicate. As previously described,[16] cell survival was measured 24 h after by MTT test; 50 μL of 0.5% MTT solution was then added in each well and incubated for 3 h at 37 °C to allow MTT metabolism. The formazan crystals were dissolved by adding 50 μL per well of 25% sodium dodecylsulfate solution and vigorous pipetting was performed. Absorbance was measured at 540 nm using a Multiskan MCC/340 plate reader (Labsystem, Cergy-Pontoise, France). Results were expressed as relative absorbance to untreated controls. Absorbance values for wells containing medium alone were substracted from the results of test wells.

5.8. Photocytotoxicity assay

Cell survival was measured 24 h after photosensitization using MTT assay. KB cells were seeded at the initial density of 2×10^4 cells mL^{-1} in 96-well microtitration plates. Forty-eight hours after plating, cells were exposed to photoactive compounds at 10^{-5} M. After 24 h incubation at 37 °C, the medium was removed, and cells were then washed three times with cold PBS and fresh RPMI was added before cell irradiation. Results are given as the percentage of the result obtained with the control cultures exposed to photosensitizer alone. Light doses, yielding 50% growth inhibition (LD_{50}), were calculated using medium effect algorithm,[34] and expressed as mean values of three independent experiments performed during different weeks. We used one plate for each dose of light from 1.5 to 15.0 J/cm^2. In order to perform the experiments exactly in the same conditions for the three photosensitizers (TPP, **1** and **2**), we divided each plate into three parts corresponding to each compound. The dark toxicity of photosensitizers was assessed separately following a similar procedure.

5.9. Light source

Irradiation was carried out at 650 nm, using a dye laser (SpectraPhysics 375B) pumped with an argon laser (Spectra-Physics 2020, Les Ulis, France). The output power was 500 mW. The light spot was 7 cm in diameter, providing the fluence rate of 13 mW/cm^2. During irradiation, the temperature never exceeded 24 ± 2 °C. This temperature did not influence cell viability.

5.10. Accumulation assay

KB cells were grown in 75 cm^2 plastic tissue culture flasks (10^5 cells mL^{-1}) in RPMI 1640 medium and incubated for 48 h at 37 °C. Under strictly subdued light conditions, the medium was then replaced with fresh folate-free RPMI 1640 medium containing 1 μM photo-active compounds. Each experiment was carried

out in the presence or absence of folic acid (4 mM). After 24 h incubation, the cells were washed twice in PBS, harvested by enzymatic disaggregation, washed in ice-cold PBS using centrifugation and the fluorescence from the drug-loaded cells was measured in 1.5 mL ethanol solution. The fluorescence intensity of each sample was normalized to cell concentration.

5.11. Statistical analysis

Mann and Whitney *U* test was used to test for the significant level between independent variables. The level of significance was set to $p < 0.05$.

Acknowledgements

This study was supported by grants from the French 'Ligue Contre le Cancer, Comités Lorrains'.

References and notes

1. Dougherty, T. J.; Gomer, C. J.; Henderson, B. W.; Jori, G.; Kessel, D.; Korberlik, M.; Moan, J.; Peng, Q. *J. Natl. Cancer Inst.* **1998**, *90*, 889.
2. Pass, H. I. *J. Natl. Cancer Inst.* **1993**, *85*, 443.
3. Jori, G. *J. Photochem. Photobiol. B Biol.* **1996**, *36*, 87.
4. Sharman, W. M.; Van Lier, J. E.; Allen, C. M. *Adv. Drug Delivery Rev.* **2004**, *56*, 53.
5. Lu, Y.; Low, P. S. *Adv. Drug Delivery Rev.* **2002**, *54*, 675.
6. Leamon, C. P.; Low, P. S. *Proc. Natl. Acad. Sci. U.S.A.* **1991**, *88*, 5572.
7. Turek, J. J.; Leamon, C. P.; Low, P. S. *J. Cell Sci.* **1993**, *106*, 423.
8. Kamen, B. A.; Capdevila, A. *Proc. Natl. Acad. Sci. U.S.A.* **1986**, *83*, 5983.
9. Frochot, C.; Di Stasio, B.; Barberi-Heyob, M.; Carré, M. C.; Zwier, J. M.; Guillemin, F.; Viriot, M. L. *Oftalmologia* **2003**, *56*, 62.
10. Saul, J. M.; Annapragada, A.; Natarajan, J. V.; Bellamkonda, R. V. *J. Controlled Release* **2003**, *92*, 49.
11. Stahl, G. L.; Walter, R.; Smith, C. W. *J. Org. Chem.* **1978**, *43*, 2285.
12. Leamon, C. P.; Pastan, I.; Low, P. S. *J. Biol. Chem.* **1993**, *269*, 24847.
13. Wang, S.; Luo, J.; Lantrip, D. A.; Waters, D. J.; Mathias, C. J.; Green, M. A.; Fuchs, P.; Low, P. S. *Bioconjugate Chem.* **1997**, *8*, 673.
14. Gabizon, A.; Horowitz, A. T.; Goren, D.; Tzemach, D.; Mandelbaum-Shavit, F.; Qazen, M. M.; Zalipsky, S. *Bioconjugate Chem.* **1999**, *10*, 289.
15. Wang, S.; Lee, R. J.; Mathias, C. J.; Green, M. A.; Low, P. S. *Bioconjugate Chem.* **1996**, *7*, 56.
16. Barberi-Heyob, M.; Vedrine, P. O.; Merlin, J. L.; Millon, R.; Abecassis, J.; Poupon, M. F.; Guillemin, F. *Int. J. Oncol.* **2004**, *24*, 951.
17. Lee, R. J.; Low, P. S. *J. Biol. Chem.* **1994**, *269*, 3168.
18. Leamon, C. P.; Copper, S. R.; Hardee, G. E. *Bioconjugate Chem.* **2003**, *14*, 738.
19. Wang, S.; Lee, R. J.; Cauchon, G.; Gorenstein, D. G.; Low, P. S. *Proc. Natl. Acad. Sci. U.S.A.* **1995**, *92*, 3318.
20. Lu, Y.; Low, P. S. *J. Controlled Release* **2003**, *91*, 17.
21. Matulic-Adamic, J.; Sanseverino, M.; Beigelman, L. *Tetrahedron Lett.* **2002**, *43*, 4439.
22. Gruner, B. A.; Weitman, S. D. *Invest. New Drugs* **1998**, *16*, 205.
23. Toffoli, G.; Russo, A.; Gallo, A.; Cernigoi, C.; Miotti, S.; Sorio, R.; Tumolo, S.; Boiocchi, M. *Int. J. Cancer* **1998**, *79*, 121.
24. Ross, J. F.; Wang, H.; Behm, F. G.; Mathew, P.; Wu, M.; Booth, R.; Ratnam, M. *Cancer* **1999**, *85*, 348.
25. Wang, S.; Low, P. S. *J. Controlled Release* **1998**, *53*, 39.
26. Franklin, W. A.; Waintrub, M.; Edwards, D.; Chistensen, K.; Prendegrast, P.; Woods, J.; Bunn, P. A.; Kolhouse, J. F. *Int. J. Cancer* **1994**, *8*, 89.
27. Kennedy, M. D.; Jallad, K. N.; Thompson, D. H.; Ben-Amotz, D.; Low, P. S. *J. Biomed. Opt.* **2003**, *8*, 636.
28. Shen, F.; Ross, J. F.; Wang, X.; Ratnam, M. *Biochemistry* **1994**, *33*, 1209.
29. Rosenthal, I. *Photochem. Photobiol.* **1991**, *53*, 859.
30. Isele, U.; Schieweck, K.; Kessler, R.; Hoogevest, P. V.; Capraro, H. G. *J. Pharm. Sci.* **1995**, *84*, 166.
31. Hornung, R. *Curr. Drug Targets Immune Endocr. Metabol. Disord.* **2001**, *1*, 165.
32. Hansen, C. B.; Hoogers, G. J.; Drenth, W. *J. Mol. Catal.* **1993**, *79*, 153.
33. Mirjolet, J. F.; Barberi-Heyob, M.; Merlin, J. L.; Marchal, S.; Etienne, M. C.; Milano, G.; Bey, P. *Br. J. Cancer* **1998**, *78*, 62.
34. Chou, T. C.; Talalay, P. Application of the Median-Effect Principle for the Assessment of Low Dose Risk of Carcinogens & for the Quantification of Synergism & Antagonism of Chemotherapeutic Agents. In *New Avenues in Developmental Cancer Chemotherapy*; Harrap, K. R., Connors, T. A., Eds; NY; 1987: pp 37–64.